Received: 3 December 2021 | Revised: 22 January 2022 | Accepted: 5 February 2022

DOI: 10.1002/bit.28060

ARTICLE

BIOTECHNOLOGY AND BIOENGINEERING WILEY

Ultra-centrifugation force in adaptive evolution changes the cell structure of oleaginous yeast *Trichosporon cutaneum* into a favorable space for lipid accumulation

Qi Liu | Minping Lu | Ci Jin | Weiliang Hou | Liao Zhao | Jie Bao

State Key Laboratory of Bioreactor Engineering, School of Biotechnology, East China University of Science and Technology, Shanghai, China

Correspondence

Jie Bao, State Key Laboratory of Bioreactor Engineering, School of Biotechnology, East China University of Science and Technology, 130 Meilong Rd, Shanghai 200237, China.
Email: jbao@ecust.edu.cn

Funding information

National Natural Science Foundation of China, Grant/Award Numbers: 21978083, 31961133006

Abstract

Microbial lipid production from lignocellulose biomass provides an essential option for sustainable and carbon-neutral supply of future aviation fuels, biodiesel, as well as various food and nutrition products. Oleaginous yeast is the major microbial cell factory but its lipid-producing performance is far below the requirements of industrial application. Here we show an ultra-centrifugation fractionation in adaptive evolution (UCF) of *Trichosporon cutaneum* based on the minor cell density difference. The lightest cells with the maximum intracellular lipid content were isolated by ultra-centrifugation fractionation in the long-term adaptive evolution. Significant changes occurred in the cell morphology with a fragile cell wall wrapping and enlarged intracellular space (two orders of magnitude increase in cell size). Complete and coordinate assimilations of all nonglucose sugars derived from lignocellulose were triggered and fluxed into lipid synthesis. Genome mutations and significant transcriptional regulations of the genes responsible for cell structure were identified and experimentally confirmed. The obtained *T. cutaneum* MP11 cells achieved a high lipid production of wheat straw, approximately five-fold greater than that of the parental cells. The study provided an effective method for screening the high lipid-containing oleaginous yeast cells as well as the intracellular products accumulating cells in general.

KEYWORDS

adaptive evolution, cell structure, lignocellulose, microbial lipid, oleaginous yeast, ultra-centrifugation

1 | INTRODUCTION

Lipid is the precursor for the synthesis of aviation hydrocarbon fuel by catalytic decarboxylation or hydrogenation cracking, and biodiesel by transesterification as future carbon-neutral biofuels, besides its various food and nutrition applications (Emery & Herdt, 1991; Sitepu et al., 2014; Willis et al., 1998). Currently, vegetable oil from soybean, rapeseed, sunflower, or palm seeds is the dominate lipid feedstock, but its quantity certainly does not meet the needs of billion tons' petroleum-derived aviation or diesel fuels (Bhatia et al., 2017). Lignocellulose biomass provides the only practical carbohydrates option for sustainable production of lipid feedstock by its wide abundance and availability. However, the lipid content and productivity of the most promising microbial cell factories, oleaginous yeasts, are still far below the requirements of industrial applications when lignocellulose is used (Slininger et al., 2016). Various methods had been tried to obtain high lipid producing oleaginous yeasts, including conventional mutations, metabolic engineering modifications, or adaptive

Qi Liu, Minping Lu, and Ci Jin equally contributed to this study.

evolution, but only limited progress were obtained (Beopoulos et al., 2008; Blazeck et al., 2014; Diaz et al., 2018; Unrean et al., 2017; Yamada et al., 2017).

Microbial lipid is an accumulative and non-secretive intracellular product, thus the direct staining or labeling methods used for quick identification and screening do not work well due to the intracellular, nonsecretive, and inert properties of microbial lipid (Hoekman et al., 2012). For a preliminary screening of general yeast cells, complicated and time-consuming procedures are required including cell mass collection, chloroform-methanol extraction, vacuum evaporation of the solvent, and lipid mass weighting (Dong et al., 2016). For screening oleaginous yeasts using lignocellulose as feedstock, more difficulties are added such as inhibitors tolerance, nonglucose sugars conversion, lignin solids shearing, and so forth (Wang et al., 2016). An effective, fast, and high-throughput screening method is crucially important for developing high lipid-producing recombinants or mutants of oleaginous yeasts.

The concept of cell sorting by centrifugation might provide a prototype of high lipid-containing cells isolation. The cell density with higher lipid content is slightly smaller than that of the cells with lower lipid content. When oleaginous yeast cells are under the ultra-centrifugation force field, the lighter cells with the higher lipid content might move slowly in the centrifugal force direction. Thus, a gradient of cells with varying lipid content might be formed. Then the lighter cells could be easily and quickly fractionated by simply pipetting the cells in the upper layer of the liquid broth in the centrifugal containers. The reinoculation of the cells in successive adaptive evolution culture could lead to an even-higher lipid content in the next-round ultra-centrifugation fractionation. This procedure could also allow the whole throughput screening of the cells by fractionating the whole culture broth. The mutant cell with significant morphological changes least likely to exist in the stock of the parental cells because the starting was inoculated from a single colony at each culture, and no super large cell was observed by microscope and staining observations in the experiment of the parental strain (Gao et al., 2014; Hu et al., 2018; Huang et al., 2011; Liu et al., 2012, 2013; Y. Wang et al., 2012; J. Wang et al., 2015, 2016; Zhang & Bao 2022). The genome sequencing of the parental *Trichosporon cutaneum* ACCC 20271 was also in a clear alignment without overlaps (Wang et al., 2016). We believe that it is highly possible that long-term ultra-centrifugal force fractionation in adaptive evolution triggered the genetic mutations and transcriptional regulation changes, or at least acted as environmental stress to induce the genomic instability and then led to the potential mutations in genome scale.

We tested this concept of ultra-centrifugation fractionation in adaptive evolution (UCF) for isolating the high lipid accumulating *T. cutaneum* cells, and evaluated the lipid production using lignocellulose (wheat straw) as feedstock. The approach started with the adaptive evolution culture (lasted for 200 days), then the ultra-centrifugation fractionation was conducted at each reinoculation of the cells. This process changed the cell morphology to a sharply enlarged size (two orders of magnitude greater than the parental) with the thinner and fragile cell wall and the higher lipid content. The genomic mutations and significant transcriptional regulations were identified. The finally obtained *T. cutaneum* MP11 was applied to lipid fermentation using wheat straw feedstock and excellent lipid production performance was obtained. This study not only yields a practical strain for cellulosic microbial lipid production but also provides a tool for screening the accumulative intracellular metabolites in general.

2 | MATERIALS AND METHODS

2.1 | Enzymes and reagents

Cellulase enzyme Cellic CTec 2.0 was purchased from Novozymes China. The filter paper activity was measured as 203.2 FPU/ml according to the NREL protocol LAP-006 (Adney & Baker, 1996), the protein concentration was 87.3 mg/ml according to Bradford method using bovine serum albumin as protein standard (Bradford, 1976). Yeast extract was purchased from Oxoid. Glucose and other solid reagents were purchased from Tianchem. Hydrochloric acid, trichloromethane, and other liquid reagents were purchased from Sinopharm Chemical Reagent.

2.2 | Microorganisms

The parental strain *T. cutaneum* ACCC 20271 was obtained from the Agricultural Culture Collection of China, Beijing, China. The whole-genome has been deposited at DDBJ/EMBL/GenBank as the accession of LTAL00000000 (Wang et al., 2016). The seed culture is yeast extract peptone dextrose (YPD) medium containing 20 g/L glucose, 20 g/L peptone, and 10 g/L yeast extract. The adaptive evolution was conducted in the synthetic medium containing 60 g/L glucose, 1.0 g/L KH_2PO_4, 0.5 g/L yeast extract, 0.5 g/L $MgSO_4$. $7H_2O$, 0.22 g/L $(NH_4)_2SO_4$.

The biodetoxification fungus *Amorphotheca resinae* ZN1 was isolated in our previous study (Zhang et al., 2010) and stored in China General Microbiological Culture Collection Center (CGMCC 7452). *A. resinae* ZN1 was firstly activated on PDA slant at 28°C for 3 days. The spores of *A. resinae* ZN1 were harvested and mixed with 200 g (wet weight) of fresh pretreated wheat straw, and then cultured at 28°C for 7 days as the seed. 10% (w/w) of seed solids were inoculated onto the freshly pretreated wheat straw and cultured at 28°C and pH 5.5 under static condition (Yi et al., 2019).

2.3 | Feedstock, pretreatment, biodetoxification, and wheat straw hydrolysate preparation

The wheat straw feedstock was harvested from Binzhou City, Shandong Province, China in summer 2018. The wheat straw was coarsely chopped, washed to remove field dirt and stones then air-dried, and milled to pass through the mesh with 10 mm in diameter

(Zhang et al., 2021). The composition of wheat straw was measured with 32.5% (w/w) of cellulose, 21.2% (w/w) of hemicellulose, and 8.1% (w/w) of ash by NREL LAP protocols (Sluiter et al., 2008, 2012).

The pre-handled wheat straw was dry acid pretreated as previously reported methods (He et al., 2014; Zhang et al., 2011). The pretreated wheat straw was neutralized by calcium hydroxide, and then biodetoxified using *A. resinae* ZN1 to remove the inhibitors as previously described (He et al., 2016; Zhang et al., 2011) without wastewater generation and solid particle loss.

The pretreated and biodetoxified wheat straw was enzymatically hydrolyzed at 20% (w/w) solids loading with the enzyme dosage of 6 mg cellulase protein per gram of dry solid matter. The hydrolysis lasted for 48 h at 50°C and pH 4.8. The wheat straw hydrolysate was centrifuged to remove the insoluble solids and added fermentation nutrients included 1.0 g/L KH_2PO_4, 0.5 g/L yeast extract, 0.5 g/L $MgSO_4$. $7H_2O$, and 0.22 g/L $(NH_4)_2SO_4$.

2.4 | Adaptive evolution under ultra-centrifugation force fractionation

T. cutaneum cells were cultured in 500 ml flasks containing 50 ml synthetic medium at 30°C, 180 rpm rotation rate for total 200 days (40 transfer times). Each transfer was conducted after culturing for 120 h, and then the broth was separated into two 50-ml centrifugation tubes (25 ml each) for ultra-centrifugation fractionation for 3 min at varying centrifugal force. After centrifugation, 5 ml of broth containing the lighter cells in the upper section of the culture were pipetted as the seed of the next round of adaptive evolution culture at inoculum size of 10% (v/v). When the ultra-centrifugation force was more than 20,000 *g*, the cells were accumulated on the upper section of the centrifugation tube as cell pellets. The cell pellets were collected and re-suspended in 5 ml of sterile water as the seed of the next round of adaptive evolution culture at inoculum size of 10% (v/v). The re-inoculated medium was cultured under the same conditions as above-mentioned protocol, till the next transfer after 120 h. The ultra-centrifugation force gradually increased with the transfer process from 1000 *g* to 45,000 *g* till most of the cells were floated on the surface of the broth and formed a cell pellet. The transfer was successively conducted for 40 times (200 days).

2.5 | Lipid fermentation

The two *T. cutaneum* strains (the parental ACCC 20271 and the mutant MP11) were activated in 100 ml flasks containing 20 ml YPD medium at 30°C, 180 rpm incubation rate for 24 h, then inoculated as the seed at the inoculum ratio of 10% (v/v).

The lipid fermentation in the wheat straw hydrolysate was conducted by separate hydrolysis and co-fermentation (SHF) in 3 L bioreactor equipped with Rushton impeller (Baoxing Biotech) containing 1 L wheat straw hydrolysate. The lipid fermentation was conducted at 30°C, 1 vvm of aeration and 600 rpm stirring. The pH was maintained at 5 by adding 4 M HCl.

The lipid fermentation using wheat straw feedstock was conducted by simultaneous saccharification and co-fermentation (SSCF). The pretreated and biodetoxified wheat straw was firstly pre-hydrolyzed to slurry at 30% (w/w) solids loading for 12 h using 4 mg cellulase protein per gram of dry matter in a 5 L bioreactor equipped with helical ribbon impeller. The lipid fermentation was started by transferring the pre-hydrolysate into the second 5 L bioreactor equipped with Rushton impeller of enhancing dissolved oxygen content at 30°C, 1 vvm of aeration, and 600 rpm stirring. The nutrients were added included 1.0 g/L KH_2PO_4, 0.5 g/L yeast extract, 0.5 g/L $MgSO_4$. 7 H_2O, 0.22 g/L $(NH_4)_2SO_4$. The pH was maintained at 5 by adding 4 M HCl.

2.6 | Lipid recovery and measurement

Dry cell mass was measured after centrifugation, washing and drying at 60°C for 24 h till constant weight. Lipid was extracted from the *T. cutaneum* cells using chloroform-methanol method as previously described (Folch et al., 1957). Extracted lipids were transesterified into fatty acid methyl esters (FAME) as previously described (Morrison & Smith, 1964). The fatty acid composition was determined by gas chromatography-mass spectrometry (GC-MS) as previously described (Hu et al., 2018).

2.7 | Cell properties measurement

Cells were ultrasonically homogenized and the intracellular acetyl-CoA and NADPH were analyzed using the Acetyl-CoA Analysis Kit and Coenzyme II Analysis Kit (Comin Biotech), respectively. Three replicates were done for each sample.

The contents of glucan and mannan in the cell wall were determined according to the protocol as previously described (Manners et al., 1973). Chitin in the cell wall was measured as previously performed (Domer, 1971).

2.8 | Whole-genome re-sequencing and qRT-PCR

The whole-genome of *T. cutaneum* MP11 was re-sequenced in Personalbio Co. DNA libraries were constructed with an insert size of 400 bp and sequenced using the Illumina NovaSeq platform.

The total RNA was extracted by Trizol reagent (RNAiso Plus, TAKARA). Reverse transcription reactions were carried out by ReverTra Ace quantitative real-time polymerase chain reaction (qPCR RT) Master Mix with gDNA Remover kit (Toyobo). Each real-time qPCR (qRT-PCR) reaction was carried out by SYBR Green Real-time PCR Master Mix kit (Toyobo) on a BioRad CFX 96. The actin gene was served as an internal control to normalize for difference in total RNA quantity. Transcription level of the gene was quantified using the formula $2^{-\Delta\Delta Ct}$.

2.9 | HPLC analysis

Glucose, xylose, furfural, 5-hydroxymethylfurfural (HMF), and acetic acid were measured as previously described (Liu et al., 2018). D-galactose, L-arabinose, and D-mannose were analyzed by HPLC (LC-20AD, refractive index detector RID-10A, Shimadzu) equipped with HPX-87P column (Bio-rad) at 80°C with the sterilized deionized water as mobile phase at a flow rate of 0.6 ml/min.

3 | RESULTS AND DISCUSSIONS

3.1 | Ultra-centrifugation fractionation in adaptive evolution (UCF) for isolating the lightest yeast cells

Centrifugation is commonly used in biolab for cell sorting and separation based on cell density differences. Here we applied the ultra-centrifugation force to fractionate the lighter cells of the oleaginous yeast *T. cutaneum* with higher lipid content based on their minor cell density difference (Figure 1). The centrifugal force was gradually increased from 1000 *g* to 45,000 *g* in a 200 days' adaptive evolution culture (40 successive transfers). The lighter *T. cutaneum* cells were accumulated in the upper layer of the culture broth at the early stage, then formed the cell pellets on the centrifugation tube wall above the broth surface at the late stage (Figure 1). The lighter cells either floated on the upper layer (early stage) or packed as the cell pellets on the upper section of the centrifugal tube wall (late stage). The lighter cells in the broth or in the pellets were pipetted as the seed of the next-round adaptive evolution culture. Gradually and consistently, the cells with the maximum lipid accumulation and survival capacity were fractionated. The results show that the intracellular lipid content increased from the initial 34.0% at the first inoculation to 55.5% at the 16th transfer (10,000 *g*), then to 71.2% at the 34th transfer (41,000 *g*). The cell mass was also increased from the initial 6.4–14.1 g/L at the 16th transfer, then to 13.9 g/L at the 34th transfer. The cells harvested after the 34th transfer were re-streaked on the petri dish for single colony isolation. The finally obtained stable cell was designated as *T. cutaneum* MP11 and stored in China General Microbiological Culture Collection Center (CGMCC, www.cgmcc.cn) with the registration number 20048.

The ultra-centrifugation fractionation of *T. cutaneum* cells was simulated by static fluid dynamics modeling (Figure S1). The calculation results show that the cell displacement in the broth of the centrifugal tubers well agreed with the experimental observations. The lighter cells moved upward in the opposite direction of ultra-centrifugation force and packed on the upper section of the tube in the short time scale of ultra-centrifugation. On the contrary, the parental *T. cutaneum* cells moved quickly to the tube wall within 12 s then slipped to the bottom along the tube wall, which was also in agreement with the experimental observation. The cell displacement modeling convinced the feasibility of ultra-centrifugation fractionation of the cells with varying intracellular lipid content.

3.2 | Morphology and structure changes of *T. cutaneum* cells after ultra-centrifugation fractionation in adaptive evolution

The *T. cutaneum* MP11 cells experienced a dramatic morphological change after the ultra-centrifugation fractionation in the long-term adaptive evolution (Figures 2 and 3). The microscope images show that the cell morphology of *T. cutaneum* MP11 in a batch-fermentation in wheat straw hydrolysate changed from an ellipsoid shape in the early stage into a longer and enlarged rod-like one at the late stage. The cells only contained limited lipid bodies when the morphology changed, then the number of lipid bodies increased and densified in cells (Figure 2). The average cell volume of *T. cutaneum* MP11 cells (9.27×10^{-15} m^3) was significantly enlarged to approximately two orders of magnitude greater than that of the parental *T. cutaneum* ACCC 20271 cells (9.70×10^{-17} m^3) (Figure S1). The

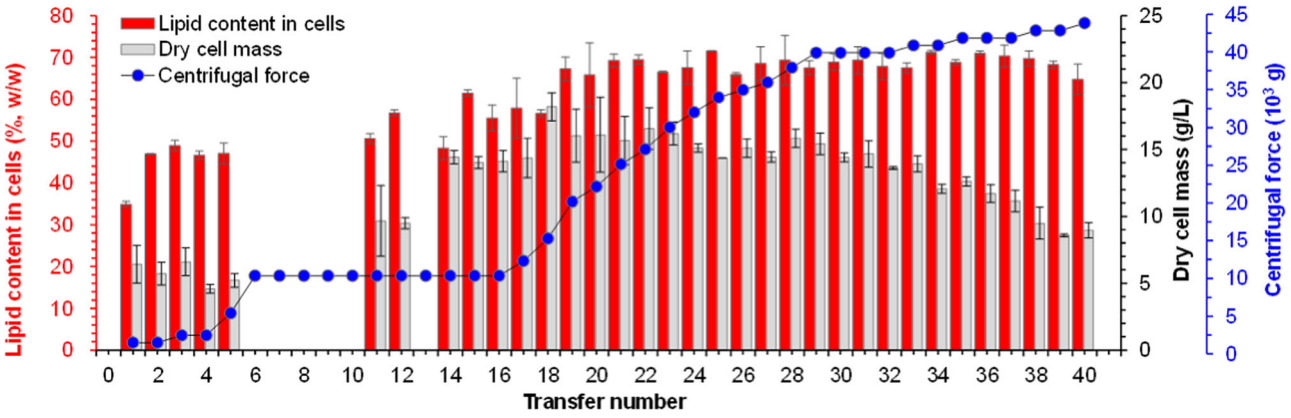

FIGURE 1 Ultra-centrifugation fractionation of *Trichosporon cutaneum* cells in adaptive evolution in flasks. Culture conditions and analysis procedures were described in Section 2 ("Microorganisms" and "Adaptive evolution under ultra-centrifugation force fractionation"). The cells in the upper layer or in the cell pellet were transferred every 5 days (120 h) by pipetting. The data during the sixth to tenth rounds were not recorded due to the temporary machine fault in cell mass measurement

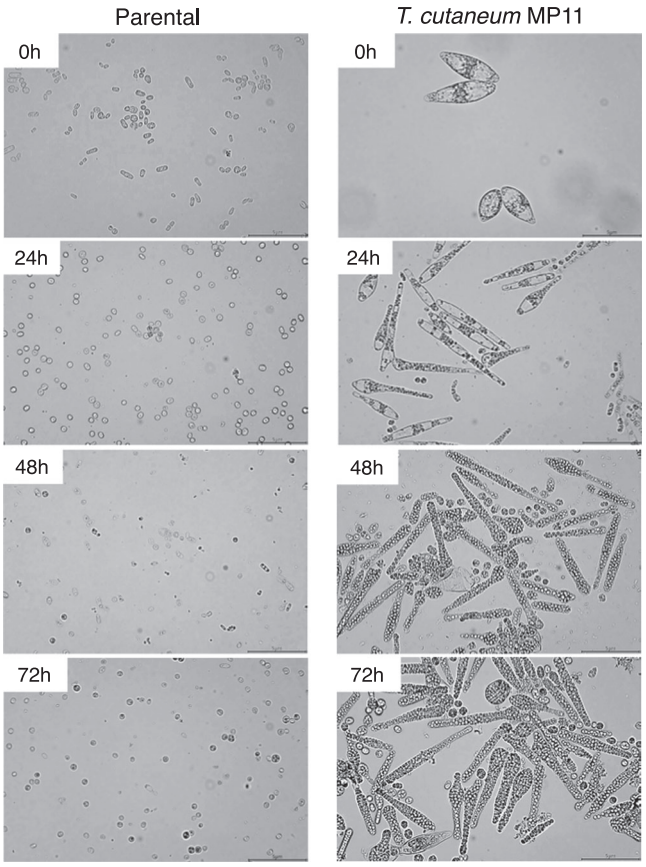

FIGURE 2 Morphology change of *Trichosporon cutaneum* cells during the batch lipid fermentation in wheat straw hydrolysate. Left, the parental cells of *T. cutaneum* ACCC 20271; Right, *T. cutaneum* MP11 cells. The fermentation was conducted in 3-L bioreactor containing 1-L wheat straw hydrolysate, 30°C, 1 vvm of aeration, and 600 rpm stirring. The microscope images were taken at 0, 24, 48, and 72 h using Olympus BX51 (Olympus Co.)

parental cells maintained the same spherical shape with low lipid content during the fermentation (Figure 2).

The fluorescence microscopy (FMI) and field emission scanning electron microscopy images (FESEM) (Figure 3a) reveal that the *T. cutaneum* MP11 cells were in the form of multicellular structure divided by the larger, septa-containing spores, clearly different from the parental cells containing smaller resting spores. The spores provided the enlarged space for intracellular lipid accumulation as well as a favorable structure to resist the external stress (Wang et al., 2019).

The cross-sections of the cells in the transmission electron microscopy (TEM) imaging (Figure 3b) further demonstrate that the lipid bodies occupied almost the complete intracellular space of *T. cutaneum* MP11. The yeast cell wall is composed of a mannan layer, an inner glucan layer with chitin and protein embedded, in which the contents of glucan and chitin determine its cell wall thickness, tensile strength, porosity, and osmotic tolerance (Ene et al., 2015). Figure 3b shows that the flagella mannan layer of *T. cutaneum* MP11 cells almost disappeared with the significant reduction of mannan contents by 90.5%; the glucan/chitin layer was obviously thinner than that of the parental cells with the reduction of glucan content by 80.3%; the chitin content of the cells was slightly decreased. The reduced glucan and mannan contents of the cell wall should play an important role in disruption of the cell wall integrity and thus created a favorable cell structure for lipid accumulation.

3.3 | Genome, transcriptional, and pathway analysis of *T. cutaneum* cells

The genome of *T. cutaneum* MP11 was re-sequenced and compared with that of the parental strain *T. cutaneum* ACCC 20271. The identified mutations included 1473 single nucleotide polymorphisms (SNPs), 945 small indel (InDels), and 124 copy number variation (CNV). The nonsynonymous mutations and copy number variations in the re-sequencing map were screened and analyzed (Table S1). Transcriptional regulation of the genes responsible for the cell structure and lipid synthesis were measured using RT-qPCR (-Figures 4 and 5).

The cell morphology changes of *T. cutaneum* MP11 was analyzed using re-sequencing (Table S1) and transcriptional (Figure S2) results. The gene Trcu_04577 encoding a subunit Sec. 8p of multiprotein exocyst complex was mutated and dramatically downregulated. Sec. 8p oversees the delivery of hydrolytic enzymes to cell septum by vesicles during cell separation of yeasts (Wang et al., 2002), thus the mutation of Trcu_04577 may be related to the formation of a multinuclear structure of *T. cutaneum* MP11 cells. Another mutant occurred on the gene Trcu_04302 encoding a subunit of protein kinase C (PKC) on regulation of stress response induced-morphogenesis and cell wall integrity (Biswas et al., 2007; Reinoso-Martín et al., 2004). Trcu_04302 was also significantly downregulated and may be responsible for the changes of cell morphology and thinness of cell wall.

The glucan and mannan contents of *T. cutaneum* MP11 were significantly reduced by 80.3% and 90.5% compared with that of the parental cells, respectively (Figure 3b). The genes Trcu_05082, Trcu_03502 encoding endoglucanases for glucan degradation, and the genes Trcu_03942, Trcu_00855 encoding mannases for mannan degradation were significantly upregulated 5.1- to 9.2-folds (-Figure 4a,b), in which the mutation of Trcu_03502 was also identified (Table S1). Trcu_00765 encoding chitin synthetase 6 was also mutated (Table S1) and downregulated (Figure 4c). These mutations and transcriptional changes might lead to the thinner glucan/chitin and mannan layer, then consequently contribute to a more fragile cell wall structure and larger cell volume for lipid accumulation (Figure 3b).

Lipid accumulation highly depends on the intracellular acetyl-CoA flux, NADPH supply, and synthesis capacity of free fatty acid and triglyceride. Figure 5a reveals that the pyruvate dehydrogenase complex genes (Trcu_00818, Trcu_03773, Trcu_02935, and Trcu_02957) were significantly upregulated, which may favor the synthesis of the lipid precursor acetyl-CoA. The isocitrate dehydrogenase (IDH) gene Trcu_00627 showed the most significant upregulation and might lead to the potential enhanced NADPH supply (Figure 5b). This phenomenon seems to be contradictory to the

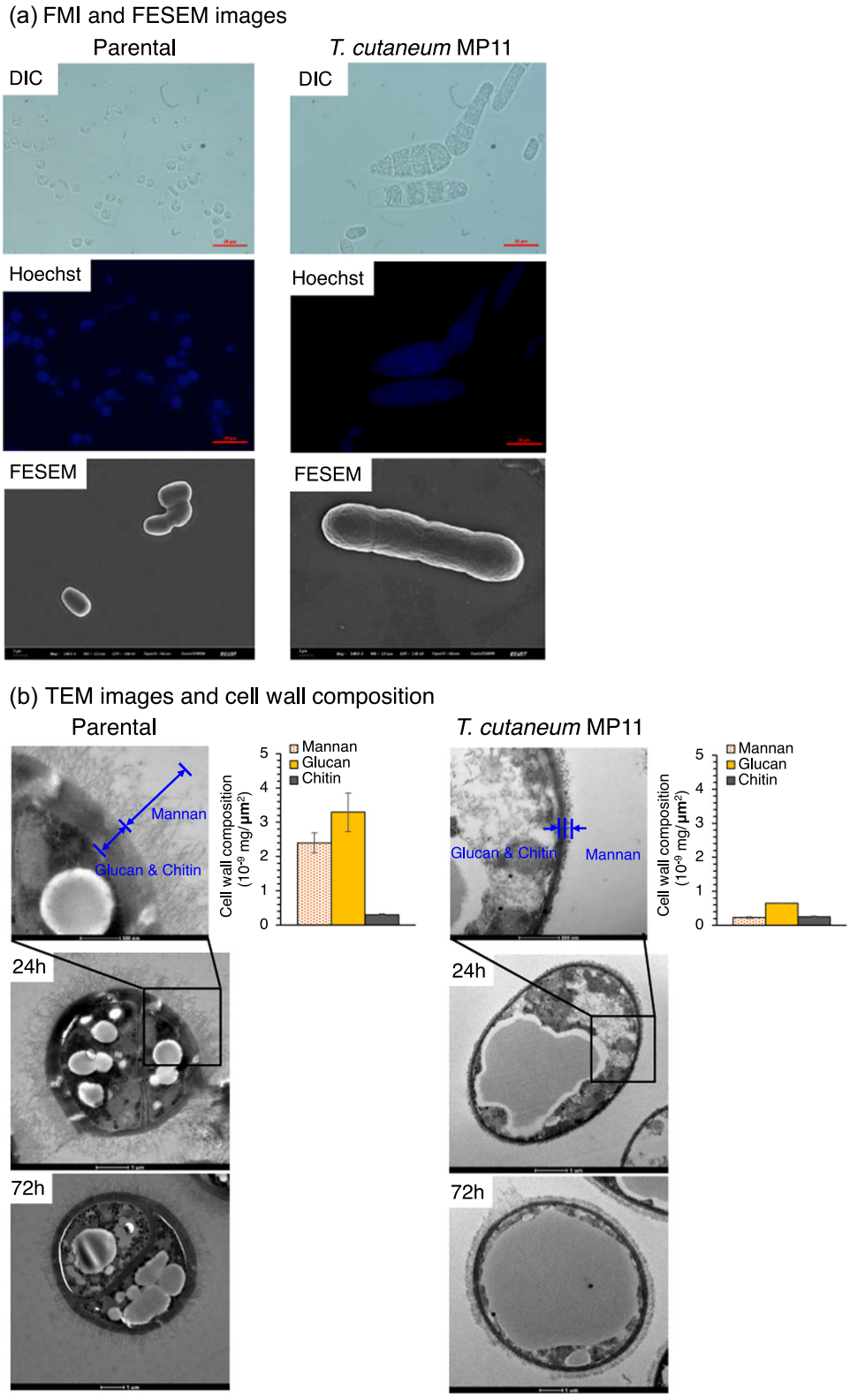

FIGURE 3 Structure changes of *Trichosporon cutaneum* cells after ultra-centrifugation fractionation in adaptive evolution. (a) Fluorescence microscopy images (FMI) and field emission scanning electron microscope (FESEM) images. For FMI, the collected cells were mixed with 4% paraformaldehyde and 0.2% Triton X-100 solution. The nucleophilic dye of Hoechst 33258 (Beyotime Biotech) was used for nuclear staining. For FESEM, the cells were collected, immobilized by 2.5% glutaraldehyde solution, dehydrated by gradient concentration ethanol solution (30%–100%), vacuum freeze drying for 12 h, and then used for imaging. (b) Transmission Electron Microscope (TEM) photos and cell wall composition of the cells before (parental strain, left) and after ultra-centrifugation fractionation in adaptive evolution (*T. cutaneum* MP11, right). Cells were harvested at 24 h and 72 h. Fresh glutaraldehyde solution was used for immobilizing collected cells. The immobilized cells were then embedded, sectioned, and stained for TEM imaging. For measurement of cell wall composition, cells were cultivated in synthetic medium at 30°C and 180 rpm incubation rate for 24 h

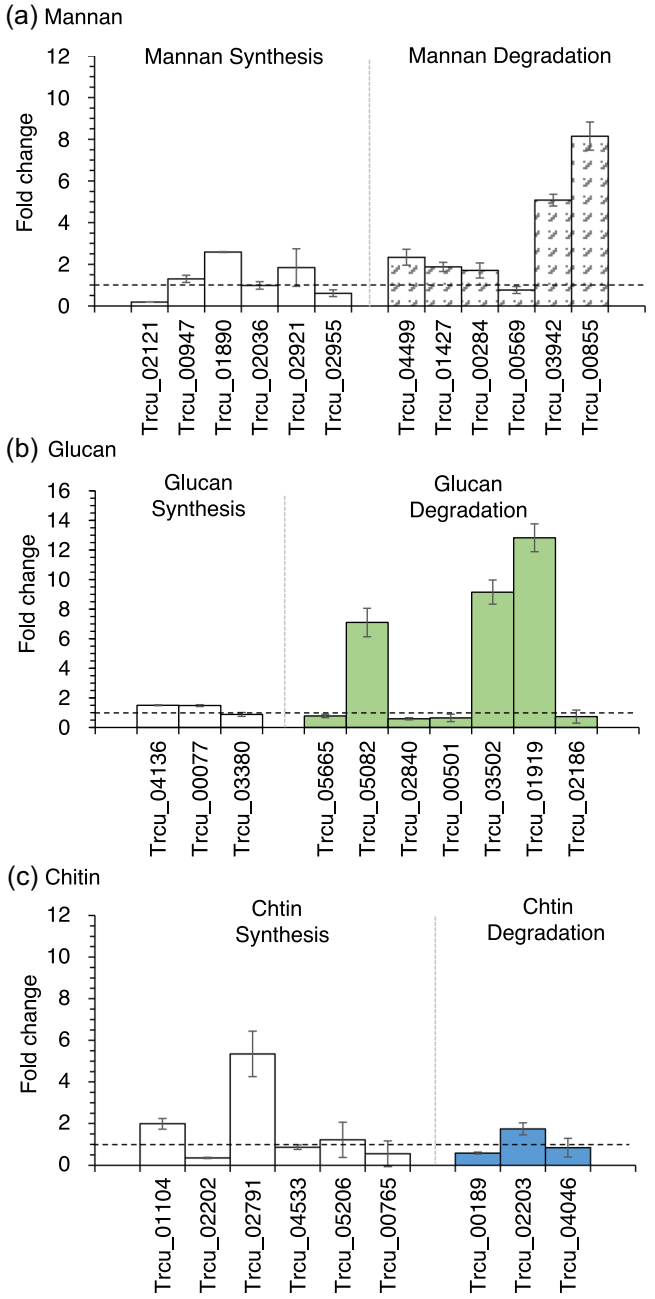

FIGURE 4 Transcriptional analysis of the genes resposible for synthesis and degradation of cell wall components of *Trichosporon cutaneum* MP11. (a) Mannan; (b) Glucan; (c) Chitin. 30-ml broth samples were collected after cultured for 24 h, then centrifuged at 8000 rpm for 5 min. The cell pellets were washed with distilled water twice and then frozen in liquid nitrogen for 10 min before mRNA extraction. The expression levels were normalized against the parental strain *T. cutaneum* ACCC 20271. Each RT-qPCR was performed at least three times. mRNA, messenger RNA; RT-qPCR, quantitative real-time polymerase chain reaction

previous results that the weak IDH activity was favorable for lipid synthesis (Yang et al., 2012). The selected genes responsible for syntheses of fatty acids and triglyceride precursors of lipid were generally upregulated (except one slight downregulated) (Figure 5c,d). Among which, the gene Trcu_03701 encoding long-chain acyl-CoA synthetase (ACSL) was upregulated 5.3-folds with a mutation occurred (Table S1). The transcriptional results were confirmed by the experimentally measured intracellular contents of NADPH (7.0-folds greater at 24 h) and acetyl-CoA (3.8-folds greater at 72 h) than that in the parental strain (Figure 5e,f), respectively. The increases of the acetyl-CoA, NADPH, free fatty acid flux, and triglyceride flux (the direct precursors of lipid) provided the positive factors for lipid synthesis in *T. cutaneum* MP11 (Figure S3).

The genome sequencing/transcription analysis provided the possible targets for metabolic engineering in *T. cutaneum* cells. However, molecular manipulation system did not work well at the present stage on this wide, nonconventional oleaginous yeast because of the difficulties in genetic manipulation (antibiotic insensitivity, inefficient homologous recombination, inefficient transformation, etc.). We are still working on an efficient gene manipulation system and metabolic engineering to upgrade the cell factory efficiency for lipid production. On the other hand, it is practically not possible to retrieve the exact time point of the mutation occurred during the ultra-centrifugation fractionation in adaptive evolution process. However, the results strongly support that the mutation occurred with the significant differences in cell morphology, dramatically enlarged intracellular space, and lipid accumulation capacity. Ultra-centrifugation force should have been played the determinative factor on triggering the mutation, or at least acted as environmental stress to induce the genomic instability before the mutations.

3.4 | Lipid production of *T. cutaneum* MP11 using lignocellulose as feedstock

The lipid fermentability of *T. cutaneum* MP11 using lignocellulose (wheat straw) as feedstock was evaluated with the parental strain *T. cutaneum* ACCC 20271 as control (Figure 6). Wheat straw was dry acid pretreated, biodetoxified, and simultaneously saccharified and co-fermented (SSCF) at 30% (w/w) solids loading as described in the Method section. *T. cutaneum* MP11 showed complete and coordinated assimilation of the full spectrum of lignocellulose-derived sugars of glucose, xylose, arabinose, galactose, and mannose (Figure 6a–d). The final lipid titer, productivity, and yield reached to 34.4 g/L, 8.6 g/L/d, and 0.22 g/g total sugars hydrolyzed from pretreated wheat straw (Figure 6e), approximately 5.0-folds greater than that of the parental strain *T. cutaneum* ACCC 20271. This yield also indicated an equivalent of approximately 10 kg lipid production from 100 kg of dry wheat straw, showing the potential of industrial practical application for future biofuels production.

Table 1 summarizes the lipid production results using typical lignocellulosic feedstocks (corn stover, wheat straw, rice straw, corncob, and palm empty fruit bunches). Only the gravitational measurement of lipid by organic solvent extraction and lipid weighting were cited, while the results by the staining method were not included. The record-high lipid content by *T. cutaneum* MP11 showed a significant elevation of lipid production (Table 1a). The

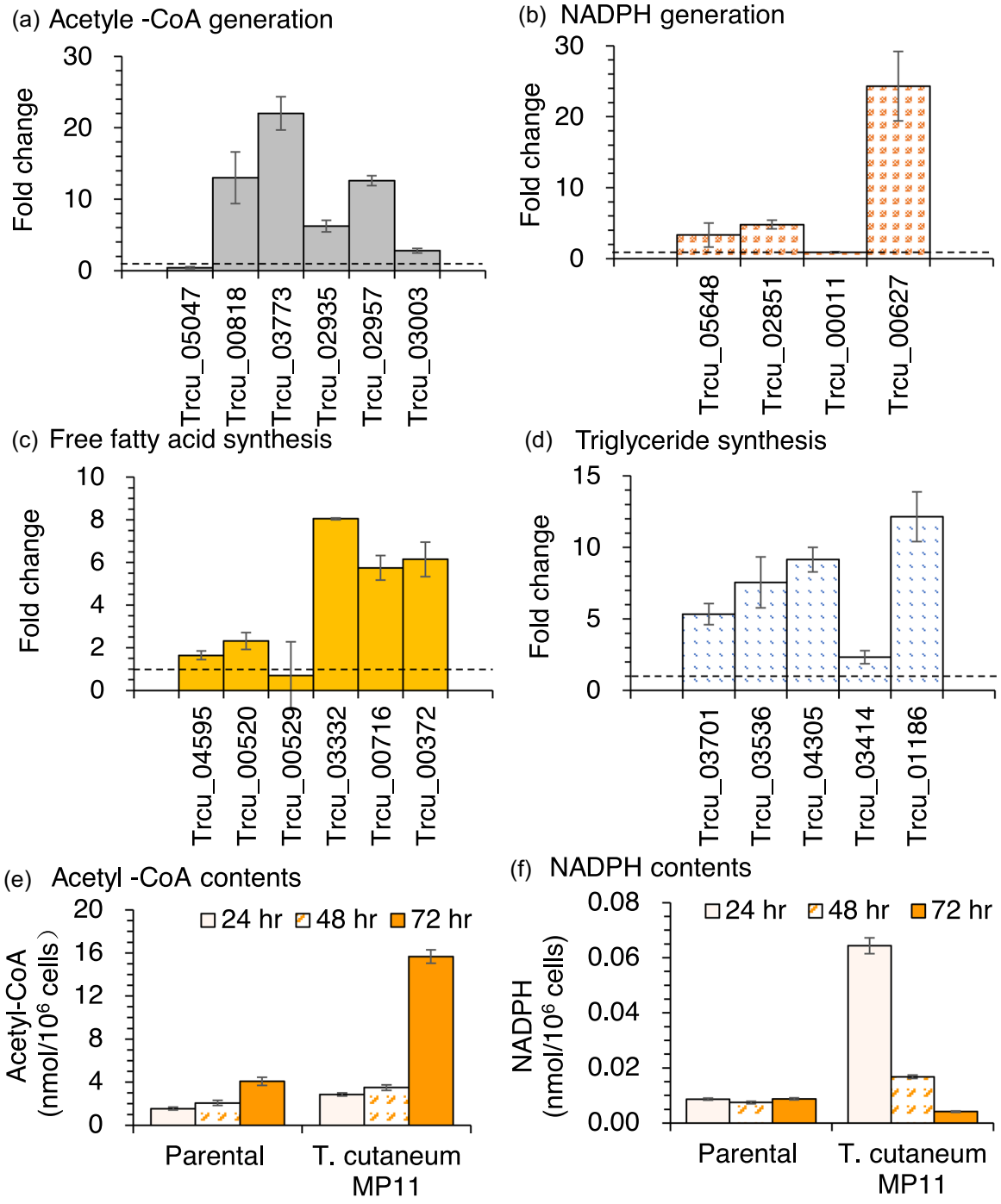

FIGURE 5 Transcriptional and intracellular metabolite analysis related to lipid synthesis. (a) Acetyle-CoA generation; (b) NADPH generation; (c) free fatty acid synthesis; (d) triglyceride synthesis; (e) experimentally measured intracellular acetyl-CoA, and (f) NADPH contents at 24, 48, and 72 h. The gene expression levels were normalized against the parental strain *Trichosporon cutaneum* ACCC 20271. Each RT-qPCR was performed at least three times. The cell samples for (e) and (f) were harvested in synthetic medium at 24, 48, and 72 h intervals. RT-qPCR, quantitative real-time polymerase chain reaction

microbial lipid fermentation performance of oleaginous yeasts using pure glucose as carbohydrates feedstock is generally better than that using lignocellulose feedstock (without fed-batch or continuous supplementation of glucose into the fermentation broth). The lipid contents in cells and lipid titer using glucose by *Rhodosporidium toruloides* Y4, *T. cutaneum* B3, and *Rhodotorula graminis* DBVPG 4620 were 62.2% and 11.2 g/L, 46.2% and 12.5 g/L, 52.2% and 7.9 g/L, respectively (Galafassi et al., 2012; Wang et al., 2019; Wu et al., 2010). When glycerol was used, the lipid content and titer by *R. toruloides* AS2.1389 were 69.5% and 18.5 g/L, respectively

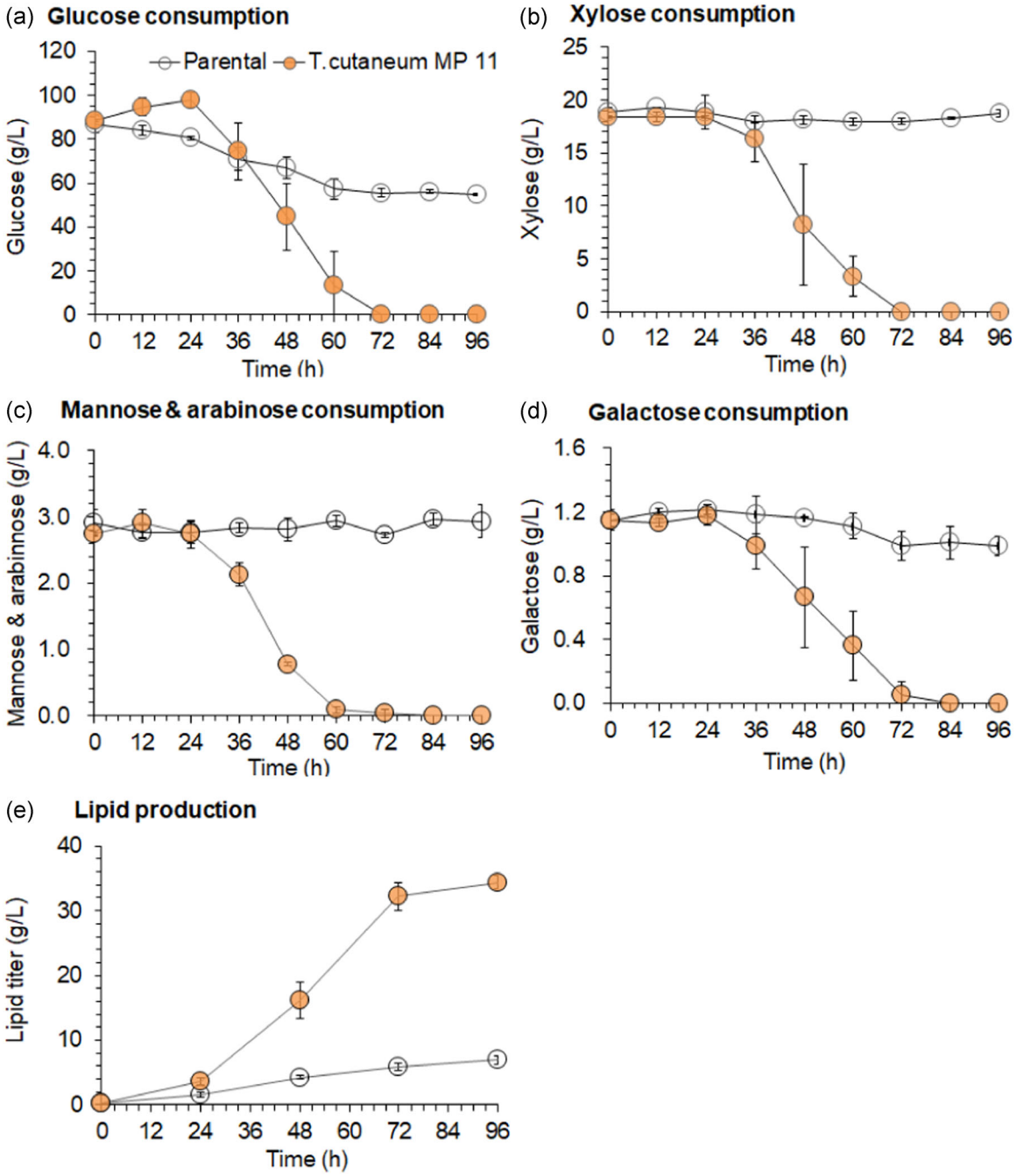

FIGURE 6 Simultaneous saccharification and co-fermentation (SSCF) of *Trichosporon cutaneum* MP11 for lipid production using wheat straw feedstock. (a) Glucose consumption; (b) xylose consumption; (c) Mannose and arabinose consumption; (d) galactose consumption; (e) lipid titer. The parental *T. cutaneum* ACCC 20271 was used as control. The residual time (~16.5 min) of mannose and arabinose peaks in HPLC with HPX-87P column and RID-10A detector was close, therefore the two were calculated as the sum of the two sugars. Pre-hydrolysis lasted for 12 h at 30% (w/w) solids loading. The seed was then inoculated at 10% (v/v) size, and the consequent SSCF was at 30°C, 180 rpm incubation rate for 96 h

(Xu et al., 2012). The present results showed an unusual exception that the lipid content and titer by *T. cutaneum* MP11 were significantly greater than that using glucose as carbohydrates (67.8% of lipid content and 34.4 g/L in titer using 30% solids loading of wheat straw).

The fatty acid compositions by *T. cutaneum* MP11 were highly similar to the general microbial lipid and vegetable oil (palmitic acid C16:0, ~30%; stearic acid C18:0, ~20%; oleic acid C18:1, ~40%) (Table 1b). The results indicate both the productivity and the quality of the lipid produced by *T. cutaneum* MP11 well met the standard of consequent catalytic decarboxylation for aviation fuels, transesterification for biodiesel, and functional food and nutrient needs.

TABLE 1 Lipid fermentation performance of various oleaginous yeasts using lignocellulose hydrolysates (without sugar concentrating)

(a) Lipid production

Feedstock	Strains	Biorefining methods	Content (%, w/w)	Titer (g/L)	Productivity (g/L/d)	Sources
Wheat straw	*Trichosporon cutaneum* MP11	Dry acid pretreatment, biodetoxification, SSF	67.8	34.4	8.6	This study
Corn stover	*T. cutaneum* ACCC 20271	Dry acid pretreatment, biodetoxification, SSF	27.0	8.1	1.1	Wang et al. (2016)
Corn stover	*Clavulina humicola* UCDFST 10-1004	AFEX pretreatment, SHF	40.0	15.5	N/A	Sitepu et al. (2013)
Corn stover	*Rhodotorula graminis* DBVPG 4620	Dilute acid pretreatment, SHF	34.0	16.3	5.4	Galafassi et al. (2012)
Corn stover	*Mortierella isabellina* ACCC 42613	Dilute acid pretreatment, SHF	34.5	4.8	1.2	Ruan et al. (2012)
Corn stover	*C. curvatus* ACCC 20509	Alkali pretreatment, water washing, SSF	N/A	15.1	4.7	Gong et al. (2014)
Wheat straw	*M. isabellina* NRRL 1757	Dilute acid hydrolysate, SHF	36.3	4.4	0.7	Zeng et al. (2013)
Wheat straw	*Cryptococcus curvatus* ACCC 20509	Dilute acid hydrolysate, overliming, SHF	33.5	5.8	0.8	Yu et al. (2011)
Corncob	*T. cutaneum* CH002	Dilute acid hydrolysate, overliming, SHF	36.0	10.4	2.1	Chen et al. (2013)
Corncob	*T. dermatis* CH007	Dilute acid pretreatment, water washing, SHF	40.1	9.8	1.4	Huang et al. (2012)
Palm empty fruit bunches	*Candida tropicalis* X37	Alkaline pretreatment, absorption and overliming, SHF	40.0	2.7	0.9	Tampitak et al. (2015)

(b) Fatty acid compositions

Feedstocks	Yeast species	Palmitic acid (C16:0)	Palmitoleic acid (C16:1)	Stearic acid (C18:0)	Oleic acid (C18:1)	Linoleic acid (C18:2)	Others	References
Wheat straw	*T. cutaneum* MP11	31.0	2.2	18.2	41.6	1.5	5.5	This study
Corn stover	*T. cutaneum* ACCC 20271	19.4	10.7	6.0	42.1	4.3	17.5	Wang et al. (2016)
Corn stover	*C. curvatus* ACCC 20509	25.3	0.6	14.6	51.1	5.9	0.6	Gong et al. (2014)
Corn stover	*M. isabellina* ACCC 42613	24.6	2.5	3.8	54.5	10.6	4.1	Ruan et al. (2012)
Corn stover	*R. graminis* DBVPG 4620	20.5	–	7.2	42.1	17.2	13.0	Galafassi et al. (2012)
Wheat straw	*M. isabellina* NRRL 1757	26.2	1.5	6.8	49.9	9.0	6.4	Zeng et al. (2013)
Wheat straw	*C. curvatus* ACCC 20509	25.9	–	15.2	47.7	6.4	4.8	Yu et al. (2011)
Corncob	*T. cutaneum* CH002	28.0	–	16.5	46.6	4.9	4.0	Chen et al. (2013)
Corncob	*T. dermatis* CH007	27.7	–	13.6	43.4	10	5.3	Huang et al. (2012)
Palm empty fruit bunches	*C. tropicalis* X37	26.2	4.8	9.5	24.7	18.5	16.3	Tampitak et al. (2015)

Note: Only the results using gravitational measurement for lipid content were cited. Gravimetric measurement indicates that the lipid in cells was extracted by organic solvent followed vacuum evaporation to remove the solvent and measured by gravimetry. AFEX, authentic ammonia fiber expansion. SHF, separate hydrolysis and fermentation.

4 | CONCLUSION

An ultra-centrifugation fractionation in adaptive evolution method for isolating the higher lipid accumulating yeast cells was designed and experimentally verified. The obtained *T. cutaneum* MP11 cells showed significantly larger cell volume, thinner cell wall, and higher lipid production than those of the parental strain. The whole-genome re-sequencing and transcription analysis revealed that the genetic mutations and transcriptional changes might lead to the multicellular structure changes of the cells. The higher contents of intracellular acetyl-CoA, NADPH, and upregulated transcriptional levels of lipid synthesis related genes provided the positive factors for lipid synthesis in *T. cutaneum* MP11. The yield and titer of cellulosic lipid from wheat straw reached 0.22 g/g total sugars and 34.4 g/L by *T. cutaneum* MP11. This method could also be applied for isolating mutant cells with intracellular metabolite accumulation (inflow cells), both lighter and heavier cells (such as polyhydroxyalkanoate-producing cells).

ACKNOWLEDGMENTS

This study was supported by the National Natural Science Foundation of China (21978083, 31961133006).

CONFLICT OF INTERESTS

The authors declare no conflict of interest.

AUTHOR CONTRIBUTIONS

Jie Bao conceived and directed the study. Qi Liu and Minping Lu performed microbial and molecular biology experiments. Ci Jin and Liao Zhao performed the microscope imaging. Weiliang Hou and Jie Bao conducted static fluid dynamics modeling. Qi Liu, Minping Lu, Ci Jin, and Liao Zhao performed the data analyses. Qi Liu, Ci Jin, and Jie Bao drafted the manuscript. All the authors edited and approved the manuscript.

DATA AVAILABILITY STATEMENT

Processed quantitative transcriptomics and whole-genome re-sequencing data are in Supplementary Data. All other supporting data are available from the corresponding author on request.

ORCID

Jie Bao http://orcid.org/0000-0001-6521-3099

REFERENCES

Adney, B., & Baker, J. (1996). *Measurement of cellulase activities*, *Laboratory Analytical Procedure No. 006*. National Renewable Energy Laboratory.

Beopoulos, A., Mrozova, Z., Thevenieau, F., Le Dall, M., Hapala, I., Papanikolaou, S., Chardot, T., & Nicaud, J. (2008). Control of lipid accumulation in the yeast *Yarrowia lipolytica*. *Applied and Environmental Microbiology*, *74*, 7779–7789. https://doi.org/10.1128/AEM.01412-08

Bhatia, S., Kim, S., Yoon, J., & Yang, Y. (2017). Current status and strategies for second generation biofuel production using microbial systems. *Energy Conversion and Management*, *148*, 1142–1156. https://doi.org/10.1016/j.enconman.2017.06.073

Biswas, S., Dijck, P., & Datta, A. (2007). Environmental sensing and signal transduction pathways regulating morphopathogenic determinants of *Candida albicans*. *Microbiology and Molecular Biology*, *71*, 348–376. https://doi.org/10.1128/MMBR.00009-06

Blazeck, J., Hill, A., Liu, L., Knight, R., Miller, J., Pan, A., Otoupal, P., & Alper, H. (2014). Harnessing *Yarrowia lipolytica* lipogenesis to create a platform for lipid and biofuel production. *Nature Communication*, *5*, 3131. https://doi.org/10.1038/ncomms4131

Bradford, M. (1976). A rapid and sensitive method for the quantitation of microgram quantities of protein utilizing the principle of protein-dye binding. *Analytical Biochemistry*, *72*, 248–254. https://doi.org/10.1016/0003-2697(76)90527-3

Chen, X., Huang, C., Yang, X., Xiong, L., Chen, X., & Ma, L. (2013). Evaluating the effect of medium composition and fermentation condition on the microbial oil production by *Trichosporon cutaneum* on corncob acid hydrolysate. *Bioresource Technology*, *143*, 18–24. https://doi.org/10.1016/j.biortech.2013.05.102

Diaz, T., Fillet, S., Campoy, S., Vazquez, R., Vina, J., Murillo, J., & Adrio, J. L. (2018). Combining evolutionary and metabolic engineering in *Rhodosporidium toruloides* for lipid production with non-detoxified wheat straw hydrolysates. *Applied Microbiology and Biotechnology*, *102*, 3287–3300. https://doi.org/10.1007/s00253-018-8810-2

Domer, J. (1971). Monosaccharide and chitin content of cell walls of *Histoplasma capsulatum* and *Blastomyces dermatitidis*. *Journal of Bacteriology*, *107*, 870–877. https://doi.org/10.1128/JB.107.3.870-877.1971

Dong, T., Knoshaug, E., Pienkos, P., & Laurens, L. (2016). Lipid recovery from wet oleaginous microbial biomass for biofuel production: A critical review. *Applied Energy*, *177*, 879–895. https://doi.org/10.1016/j.apenergy.2016.06.002

Emery, R. S., & Herdt, T. H. (1991). Lipid nutrition. *Veterinary Clinics of North America Food Animal Practice*, *7*, 341–352. https://doi.org/10.1016/S0749-0720(15)30799-4

Ene, I., Walker, L., Schiavone, M., Lee, K., Martin-Yken, H., Dague, E., Gow, N., Munro, C., & Browna, A. (2015). Cell wall remodeling enzymes modulate fungal cell wall elasticity and osmotic stress resistance. *mBio*, *6*, e00986. https://doi.org/10.1128/mBio.00986-15

Folch, J., Lees, M., & Stanley, G. (1957). A simple method for the isolation and purification of total lipides from animal tissues. *Journal of Biological Chemistry*, *226*, 497–509. https://doi.org/10.1016/s0021-9258(18)64849-5

Galafassi, S., Cucchetti, D., Pizza, F., Franzosi, G., Bianchi, D., & Compagno, C. (2012). Lipid production for second generation biodiesel by the oleaginous yeast *Rhodotorula graminis*. *Bioresource Technology*, *111*, 398–403. https://doi.org/10.1016/j.biortech.2012.02.004

Gao, Q., Cui, Z., Zhang, J., & Bao, J. (2014). Lipid fermentation of corncob residues hydrolysate by oleaginous yeast *Trichosporon cutaneum*. *Bioresource Technology*, *152*, 552–556. https://doi.org/10.1016/j.biortech.2013.11.044

Gong, Z., Shen, H., Yang, X., Wang, Q., Xie, H., & Zhao, Z. (2014). Lipid production from corn stover by the oleaginous yeast *Cryptococcus curvatus*. *Biotechnology for Biofuels*, *7*, 158. https://doi.org/10.1186/s13068-014-0158-y

He, Y., Zhang, J., & Bao, J. (2014). Dry dilute acid pretreatment by co-currently feeding of corn stover feedstock and dilute acid solution without impregnation. *Bioresource Technology*, *158*, 360–364. https://doi.org/10.1016/j.biortech.2014.02.074

He, Y., Zhang, J., & Bao, J. (2016). Acceleration of biodetoxification on dilute acid pretreated lignocellulose feedstock by aeration and the consequent ethanol fermentation evaluation. *Biotechnology for Biofuels*, *9*, 19. https://doi.org/10.1186/s13068-016-0438-9

Hoekman, S., Broch, A., Robbins, C., Ceniceros, E., & Natarajan, M. (2012). Review of biodiesel composition, properties, and specifications.

Renewable and Sustainable Energy Reviews, *16*, 143–169. https://doi.org/10.1016/j.rser.2011.07.143

Hu, M., Wang, J., Gao, Q., & Bao, J. (2018). Converting lignin derived phenolic aldehydes into microbial lipid by *Trichosporon cutaneum*. *Journal of Biotechnology*, *281*, 81–86. https://doi.org/10.1016/j.jbiotec.2018.06.341

Huang, C., Chen, X., Xiong, L., Chen, X., & Ma, L. (2012). Oil production by the yeast *Trichosporon dermatis* cultured in enzymatic hydrolysates of corncobs. *Bioresource Technology*, *110*, 711–714. https://doi.org/10.1016/j.biortech.2012.01.077

Huang, X., Wang, Y., Wei, L., & Bao, J. (2011). Biological removal of inhibitors leads to the improved lipid production in the lipid fermentation of corn stover hydrolysate by *Trichosporon cutaneum*. *Bioresource Technology*, *102*, 9705–9709. https://doi.org/10.1016/j.biortech.2011.08.024

Liu, G., Zhang, Q., Li, H., Qureshi, A. S., Zhang, J., Bao, X., & Bao, J. (2018). Dry biorefining maximizes the potentials of simultaneous saccharification and co-fermentation for cellulosic ethanol production. *Biotechnology and Bioengineering*, *115*, 60–69. https://doi.org/10.1002/bit.26444

Liu, W., Wang, Y., Yu, Z., & Bao, J. (2012). Simultaneous saccharification and microbial lipid fermentation of corn stover by oleaginous yeast *Trichosporon cutaneum*. *Bioresource Technology*, *118*, 13–18. https://doi.org/10.1016/j.biortech.2012.05.038

Liu, Z., Gao, Y., Chen, J., Imanaka, T., Bao, J., & Hua, Q. (2013). Analysis of metabolic fluxes for better understanding of mechanisms related to lipid accumulation in oleaginous yeast *Trichosporon cutaneum*. *Bioresource Technology*, *130*, 144–151. https://doi.org/10.1016/j.biortech.2012.12.072

Manners, D., Masson, A., & Patterson, J. (1973). The structure of a beta-(1-6)-D-glucan from yeast cell walls. *Biochemical Journal*, *135*, 19–30. https://doi.org/10.1042/bj1350019

Morrison, W., & Smith, L. (1964). Preparation of fatty acid methyl esters and dimethylacetals from lipids with boron fluoride–methanol. *Journal of Lipid Research*, *5*, 600–608. https://doi.org/10.1016/s0022-2275(20)40190-7

Reinoso-Martín, C., Schüller, C., Schuetzer-Muehlbauer, M., & Kuchler, K. (2004). The yeast protein kinase C cell integrity pathway mediates tolerance to the antifungal drug caspofungin through activation of slt2p mitogen-activated protein kinase signaling. *Eukaryotic Cell*, *2*, 1200–1210. https://doi.org/10.1128/EC.2.6.1200-1210.2003

Ruan, Z., Zanotti, M., Wang, X., Ducey, C., & Liu, Y. (2012). Evaluation of lipid accumulation from lignocellulosic sugars by *Mortierella isabellina* for biodiesel production. *Bioresource Technology*, *110*, 198–205. https://doi.org/10.1016/j.biortech.2012.01.053

Sitepu, I., Garay, L., Sestric, R., Levin, D., Block, D., German, J., & Boundy-Mills, K. (2014). Oleaginous yeasts for biodiesel: current and future trends in biology and production. *Biotechnology Advance*, *32*, 1336–1360. https://doi.org/10.1016/j.biotechadv.2014.08.003

Sitepu, I., Sestric, R., Ignatia, L., Levin, D., German, J., Gillies, L., Almada, G., & Boundy-Mills, K. (2013). Manipulation of culture conditions alters lipid content and fatty acid profiles of a wide variety of known and new oleaginous yeast species. *Bioresource Technology*, *144*, 360–369. https://doi.org/10.1016/j.biortech.2013.06.047

Slininger, P., Dien, B., Kurtzman, C., Moser, B., Bakota, E., Thompson, S., Bryan, P., Cotta, M., Balan, V., Jin, M., Sousa, l, & Dale, B. (2016). Comparative lipid production by oleaginous yeasts in hydrolyzates of lignocellulosic biomass and process strategy for high titers. *Biotechnology and Bioengineering*, *113*, 1676–1690. https://doi.org/10.1002/bit.25928

Sluiter, A., Hames, B., Ruiz, R., & Scarlata, C. (2008). Determination of sugars, byproducts, and degradation products in liquid fraction process samples. NREL/TP-510-42623. National Renewable Energy Laboratory.

Sluiter, A., Hames, B., Scarlata, C., Sluiter, J., & Templeton, D. (2012). Determination of structural carbohydrates and lignin in biomass national renewable. NREL/TP-510-42618. National Renewable Energy Laboratory.

Tampitak, S., Louhasakul, Y., Cheirsilp, B., & Prasertsan, P. (2015). Lipid production from hemicellulose and holocellulose hydrolysate of palm empty fruit bunches by newly isolated Oleaginous yeasts. *Applied Biochemistry and Biotechnology*, *176*, 1801–1814. https://doi.org/10.1007/s12010-015-1679-y

Unrean, P., Khajeeram, S., & Champreda, V. (2017). Combining metabolic evolution and systematic fed-batch optimization for efficient single-cell oil production from sugarcane bagasse. *Renewable Energy*, *111*, 295–306. https://doi.org/10.1016/j.renene.2017.04.018

Wang, H., Tang, X., Liu, J., Trautmann, S., Balasundaram, D., McCollum, D., & Balasubramanian, M. (2002). The multiprotein exocyst complex is essential for cell separation in *Schizosaccharomyces pombe*. *Molecular Biology of the Cell*, *13*, 515–529. https://doi.org/10.1091/mbc.01-11-0542

Wang, J., Gao, Q., & Bao, J. (2016). Genome sequence of *Trichosporon cutaneum* ACCC 20271: An oleaginous yeast with excellent lignocellulose derived inhibitor tolerance. *Journal of Biotechnology*, *228*, 50–51. https://doi.org/10.1016/j.jbiotec.2016.04.043

Wang, J., Gao, Q., Zhang, H., & Bao, J. (2016). Inhibitor degradation and lipid accumulation potentials of oleaginous yeast *Trichosporon cutaneum* using lignocellulose feedstock. *Bioresource Technology*, *218*, 892–901. https://doi.org/10.1016/j.biortech.2016.06.130

Wang, J., Zhang, H., & Bao, J. (2015). Characterization of inulin hydrolyzing enzyme(s) in oleaginous yeast *Trichosporon cutaneum* in consolidated bioprocessing of microbial lipid fermentation. *Applied Biochemistry and Biotechnology*, *177*, 1083–1098. https://doi.org/10.1007/s12010-015-1798-5

Wang, Y., Liu, W., & Bao, J. (2012). Repeated batch fermentation with water recycling and cell separation for microbial lipid production. *Frontier of Chemical Science and Engineering*, *6*, 453–460. https://doi.org/10.1007/s11705-012-1210-8

Wang, Y., Yan, R., Tang, L., Zhu, L., Zhu, D., & Bai, F. (2019). Dimorphism of *Trichosporon cutaneum* and impact on its lipid production. *Biotechnology for Biofuels*, *12*, 203. https://doi.org/10.1186/s13068-019-1543-3

Willis, W. M., Lencki, R. W., & Marangoni, A. G. (1998). Lipid modification strategies in the production of nutritionally functional fats and oils. *Critical Reviews in Food Science and Nutrition*, *38*, 639–674. https://doi.org/10.1080/10408699891274336

Wu, S., Hu, C., Jin, G., Zhao, X., & Zhao, Z. K. (2010). Phosphate-limitation mediated lipid production by *Rhodosporidium toruloides*. *Bioresource Technology*, *101*, 6124–6129. https://doi.org/10.1016/j.biortech.2010.02.111

Xu, J., Zhao, X., Wang, W., Wei, D., & Liu, D. (2012). Microbial conversion of biodiesel byproduct glycerol to triacylglycerols by oleaginous yeast *Rhodosporidium toruloides* and the individual effect of some impurities on lipid production. *Biochemical Engineering Journal*, *65*, 30–36. https://doi.org/10.1016/j.bej.2012.04.003

Yamada, R., Yamauchi, A., Kashihara, T., & Ogino, H. (2017). Evaluation of lipid production from xylose and glucose/xylose mixed sugar in various oleaginous yeasts and improvement of lipid production by UV mutagenesis. *Biochemical Engineering Journal*, *128*, 76–82. https://doi.org/10.1016/j.bej.2017.09.010

Yang, F., Zhang, S., Zhou, Y. J., Zhu, Z., Lin, X., & Zhao, Z. K. (2012). Characterization of the mitochondrial NAD+-dependent isocitrate dehydrogenase of the oleaginous yeast *Rhodosporidium toruloides*. *Applied Microbiology and Biotechnology*, *94*, 1095–1105. https://doi.org/10.1007/s00253-011-3820-3

Yi, X., Gao, Q., Zhang, L., Wang, X., He, Y., Hu, F., Zhang, J., Zou, G., Yang, S., Zhou, Z., & Bao, J. (2019). Heterozygous diploid structure of *Amorphotheca resinae* ZN1 contributes efficient biodetoxification on solid pretreated corn stover. *Biotechnology for Biofuels*, *12*, 126. https://doi.org/10.1186/s13068-019-1466-z

Yu, X., Zheng, Y., Dorgan, K. M., & Chen, S. (2011). Oil production by oleaginous yeasts using the hydrolysate from pretreatment of wheat straw with dilute sulfuric acid. *Bioresource Technology*, *102*, 6134–6140. https://doi.org/10.1016/j.biortech.2011.02.081

Zeng, J., Zheng, Y., Yu, X., Yu, L., Gao, D., & Chen, S. (2013). Lignocellulosic biomass as a carbohydrate source for lipid production by *Mortierella isabellina*. *Bioresource Technology*, *128*, 385–391. https://doi.org/10.1016/j.biortech.2012.10.079

Zhang, B., Khushik, F. A., Zhan, B., & Bao, J. (2021). Transformation of lignocellulose to starch-like carbohydrates by organic acid-catalyzed pretreatment and biological detoxification. *Biotechnology and Bioengineering*, *118*, 4105–4118. https://doi.org/10.1002/bit.27887

Zhang, J., Wang, X., Chu, D., He, Y., & Bao, J. (2011). Dry pretreatment of lignocellulose with extremely low steam and water usage for bioethanol production. *Bioresource Technology*, *102*, 4480–4488. https://doi.org/10.1016/j.biortech.2011.01.005

Zhang, J., Zhu, Z., Wang, X., Wang, N., Wang, W., & Bao, J. (2010). Biodetoxification of toxins generated from lignocellulose pretreatment using a newly isolated fungus, *Amorphotheca resinae* ZN1, and the consequent ethanol fermentation. *Biotechnology for Biofuels*, *3*, 26. https://doi.org/10.1186/1754-6834-3-26

Zhang, Y., & Bao, J. (2022). Tolerance of *Trichosporon cutaneum* to lignin derived phenolic compounds facilitates the cell growth and cellulosic lipid accumulation. *Journal of Biotechnology*, *343*, 32–37. https://doi.org/10.1016/j.jbiotec.2021.09.009

SUPPORTING INFORMATION

Additional supporting information may be found in the online version of the article at the publisher's website.

How to cite this article: Liu, Q., Lu, M., Jin, C., Hou, W., Zhao, L., & Bao, J. (2022). Ultra-centrifugation force in adaptive evolution changes the cell structure of oleaginous yeast *Trichosporon cutaneum* into a favorable space for lipid accumulation. *Biotechnology and Bioengineering*, 119, 1509–1521. https://doi.org/10.1002/bit.28060